



VICTORIA UNIVERSITY
MELBOURNE AUSTRALIA

Sunlight-Transmitting Photocatalytic Membrane for Reduced Maintenance Water Treatment

This is the Accepted version of the following publication

Nyamutswa, Lavern Tendayi, Hanson, Blair, Navaratna, Dimuth, Collins, Stephen F, Linden, Karl G and Duke, Mikel (2021) Sunlight-Transmitting Photocatalytic Membrane for Reduced Maintenance Water Treatment. ACS ES&T Water, 1 (9). pp. 2001-2011. ISSN 2690-0637

The publisher's official version can be found at
<https://pubs.acs.org/doi/pdf/10.1021/acsestwater.1c00073>
Note that access to this version may require subscription.

Downloaded from VU Research Repository <https://vuir.vu.edu.au/42644/>

Sunlight-transmitting photocatalytic membrane for reduced maintenance water treatment

Lavern T. Nyamutswa ^a, Blair Hanson^c, Dimuth Navaratna ^{a, b}, Stephen F. Collins ^b, Karl G. Linden^c and Mikel C. Duke ^{a, *}

^a *Institute for Sustainable Industries and Liveable Cities, Victoria University, 70-104 Ballarat Road, Footscray, VIC, 3011, Australia*

^b *College of Engineering and Science, Victoria University, 70-104 Ballarat Road, Footscray, VIC, 3011, Australia*

^c *Department of Civil, Environmental, and Architectural Engineering, University of Colorado Boulder, 4001 Discovery Drive, Boulder, CO 80303, USA*

** Corresponding author: Mikel C. Duke (email: mikel.duke@vu.edu.au)*

Abstract

Membranes remove contaminants from drinking water, but require routine cleaning with harsh chemicals that are less conveniently accessed, handled, and disposed of in remote communities. This work demonstrates a non-chemical solar cleaning alternative using simulated sunlight that has been conveniently directed through a light-transmitting porous glass substrate to a thin TiO₂ photocatalytic membrane coating. Dead-end filtration of non-potable water with routine chemical-free backwashing showed the solar cleaning provided a 4.5-fold extension to the time needed before a chemical clean, as well as a 50% reduction in filtration pump electricity demand. These improvements were attributed to formation of hydroxyl radicals and subsequent oxidation of organic foulants, as well as the well-known photocatalytic superhydrophilic surface stimulation of TiO₂ surfaces. Both effects acted together to reduce irreversible surface attachment of organic foulants. Size exclusion chromatography (SEC) indicated the effect only targeted the organic molecule-membrane surface interaction as little change was observed to bulk organics profiles. Substrate light transmission onto photocatalytic membrane surfaces demonstrated in this work could be successfully applied as a membrane cleaning method during water treatment in remote communities. Future explorations can be made into potential for enhanced disinfection and anti-fouling functions on wider ranges of organic contaminated water supplies.

Keywords

Photocatalytic membrane, anti-fouling, water treatment, solar energy, photocatalysis, self-cleaning

Synopsis

A demonstration of sunlight facilitated photocatalysis and through-substrate light transmission as an alternative method for cleaning membranes during water filtration.

1. Introduction

While membrane technology is now widely applied to improve the quality and safety of drinking water supply, further innovative solutions are still required, for example, in remote or disadvantaged communities which must consider the lack of resources, expertise as well as reliable transport and communication networks ¹. Membrane filtration can be sustainably adopted for most of the remote water treatment needs if the use of one of its biggest consumables needed to combat fouling from water born contaminants, cleaning chemicals, is minimised or eliminated ².

Adopting fouling controls that minimise chemical use could lead to practically viable applications of membrane technologies for providing clean water to remote communities. Among these fouling control methods are operational interventions which contribute in removing the fouling layer, such as physical cleaning of the membrane, backwashing and relaxation of the filtration process, as well as fabrication interventions such as modification of the membrane surface ³. In spite of these interventions, foulants strongly bound to membrane surfaces eventually need to be removed through intensive chemical cleaning routines, such as frequent (hourly-weekly) chemically enhanced backwashing (CEB) and less frequent (quarterly-annually) and more intensive clean-in-place (CIP) procedures ⁴. Fouling control is also important for keeping filtration resistance low, thus reducing the energy needed by pumps to drive water through the filtration system ⁵.

Modification of the membrane surface is aimed at tuning the surface to have less propensity for fouling. This is usually achieved by introducing hydrophilic functionality as a passive

means to prevent organic foulant deposition ³. Active fouling reduction is a more advanced means of reducing fouling with enhanced user controllability to reduce maintenance. This can be achieved by controlled switching of surface chemistry, for example by changing operation temperature ⁶ or by targeted surface reactions to foulants ⁷. Active anti-fouling functionality can also be introduced to the membrane by modification of its surface with photocatalytically active titanium dioxide (TiO₂) ⁸⁻¹⁰. Such surfaces have the so-called “self-cleaning” property, because they are capable of preventing fouling through photocatalytic reactions and induced superhydrophilicity during exposure to light energy of the correct wavelength and intensity ^{11, 12}, including sunlight. Induced super hydrophilicity is initiated when, upon irradiation, a photo-generated hole weakens the binding energy between a Ti atom and the lattice oxygen atom. This allows water molecules adsorbed to the membrane surface to break the weakened Ti–O–Ti bonds, forming two new Ti–OH bonds ¹³. With more water molecules adsorbing to the hydroxyl group through van der Waals forces and hydrogen bonding, the surface becomes even more hydrophilic, achieving superhydrophilic status, which increases hydrophobic contaminants anti-fouling ¹⁴. Induced superhydrophilicity also reduces membrane resistance to water permeation, contributing to lowering of pump energy requirements for water filtration.

Photocatalytic membranes have shown superior anti-fouling properties and ability to degrade pollutants and disinfect water through a series of photocatalytic oxidation reactions initiated by reactive oxygen species (ROS) ¹³. ROS include hydroxyl and superoxide radicals, where the former is a powerful oxidant capable of degrading even some of the most recalcitrant organic water pollutants ^{15, 16}. The hydroxyl radical is capable of oxidising aromatic and olefinic compounds through addition to carbon double bonds, and aliphatic compounds through hydrogen abstraction from carbon-hydrogen bonds ¹⁷.

Practical limitations and inefficiencies, however, have been identified in the traditional way that light is supplied to the photocatalytic membrane surface, especially while contained within

a membrane module ^{18, 19}. These issues include light attenuation by the concentrated feed stream, and the practical limitations of where to place artificial light sources inside the module, such as light emitting diodes (LEDs) and ultra-violet (UV) lamps. Introducing natural sunlight faces similar practicality issues. In an attempt to resolve the membrane and module limitations, we showed how light transmitting sintered glass membrane substrates can be adopted to solve these challenges ^{20, 21}. Light conducting substrates are new to membrane science, and could give the possibility of solving the challenge of introducing a light source from outside the module (e.g. sunlight or artificial UV source) to the catalyst coating, whereby light directed from the outside (towards the end and/or side) of the membrane element enclosed in a transparent (glass or polymer) housing allows light to be transmitted through the substrate along its entire length while simultaneously distributing light (e.g. by light scattering) to the entire membrane's photocatalyst coating. This is especially viable in the industry standard ceramic membrane monolith format, where its end and sides can be simply exposed to the sun within a transparent housing to "illuminate" the entire substrate and distribute/scatter light to the entire photocatalytic membrane surface. However unlike the current generation of opaque membrane materials, light-transmitting substrates must also satisfy the required mechanical strength property, thus currently limiting them to transparent materials such as glass or specific transparent polymers. Our prior work validated this concept using a 365 nm UV LED light source, which is within the specific wavelength range needed to activate the photocatalytic reactions by TiO₂, on readily available porous glass discs which we coated with sintered commercial TiO₂ particles. UV light was effectively distributed to the TiO₂ coating over porous glass via a quartz window mounted on the permeate side, and led to significant improvement to filtration performance in the presence of model foulants ²¹. However, for proving the real potential, the concept must now be demonstrated for real solar application where UV proportion in natural sunlight is minor. Further, a real surface water mimicking a possible

supply to a remote community must be demonstrated since fouling can be more complex than what model fouling testing can initially verify. This paper therefore presents the first test of the membrane's anti-fouling performance using sunlight from a solar simulator while treating a real, non-potable surface water source.

In order to continue exploring the effect from our previous UV light validation, we extended our investigation in the present study by an analysis of the hydroxyl radical generation, being evidence to photocatalytic activity that can be responsible for degrading surface attached organic foulants. Further, high performance size exclusion chromatography (HPSEC) was utilised to characterise the dissolved organic matter (DOM) in feed and treated water samples to not only understand their organic component profile, but to help explain the anti-fouling behaviour. HPSEC isolates the components of DOM that are ubiquitous in surface and ground water into its fractions containing biopolymers, humic and fulvic acids with relatively high apparent molecular weight (AMW), as well as other lower AMW compounds that include proteins and carbohydrates^{22, 23}.

As complete mineralisation of DOM compounds into carbon dioxide and water is practically impossible^{24, 25}, degradation to lower AMW compounds occurs. The size of DOM compounds can be an important factor that influences the type and extent of fouling^{26, 27}. The extent of the effectiveness of photocatalysis in membrane fouling control can therefore be determined by measuring the AMW of the feed, permeate and reject by HPSEC. Monitoring the AMW of DOM is also important because it strongly influences the reactivity of DOM in aquatic systems²². Therefore, another key feature of this study involved exploring how photocatalytic action could impact DOM and membrane performance to gain a clearer understanding of how the novel photocatalytic membrane provides beneficial operation.

2. Materials and methods

2.1. Chemicals

All chemicals used were analytical grade and used as received. A list of the chemicals used is given in SI Text S1.

2.2. Membrane fabrication and measurement of optical properties

The membranes were prepared via dip coating sintered glass substrates with a suspension of Degussa P25 TiO₂ in water and sodium alginate, followed by air drying and sintering, which is a known to be a durable inorganic particle bonding method⁵⁶. The method is described in detail in previously reported work²¹. In brief, the method involved mixing 5 g TiO₂ powder with 60 mL water and 0.4 g sodium alginate to act as a binder, followed by high-speed homogenisation and sonication to remove lumps and air bubbles. The sintered glass substrates were then mechanically dipped into the suspension, followed by air drying for 12 h and heating in a muffle furnace to 450° C at a rate of 1° C/min. Cooling was at the same slow rate to prevent cracking, followed by washing in DI water and drying at 80° C for 2 h. Successful uniform coating of TiO₂ on the substrate was confirmed by a combination of gravimetric and visual inspections, as well as scanning electron microscopy (SEM) and Energy Dispersive Spectroscopy (EDS), as reported in previous work^{20,21}.

The spectra of light between 340 nm and 400 nm passing through the substrate were obtained using a Maya 2000 PRO radiometer from Ocean Insight (Tampa, FL, USA).

2.3. Water source and membrane filtration experiments

Surface water was sampled from Boulder Creek, Boulder Colorado, USA, at a depth of 10-20 cm below the water surface. Visually, the collected water appeared largely clear and colourless, with visibly large particle suspensions. No obvious odour from the water was detected. Samples were coarse filtered through 1.5 μm Whatman glass fibre filters to remove large particulates, and stored in amber bottles at 4°C. The water was used within 3 days of collection. The water was warmed to ambient temperature and shaken to resuspend any sediments prior to being used. Filtration experiments were conducted in a custom-made stainless steel filtration module with a quartz window on the permeate side to allow entry of sunlight. Dead-end filtration of the feed water was conducted at 24°C at constant flux of 300 L/m²/h with backwashing every hour using 15mL of permeate. The filtration experiments are described further in SI Text S2.

The membrane's anti-fouling ability was evaluated by recording the trans-membrane pressure (TMP). TMP was monitored and presented as relative pressure, P/P_0 , being the ratio of the present TMP to the TMP measured at time zero of the test. The hydraulic cleaning efficiency (HCE) and the hydraulically irreversible fouling index (HIFI) were also calculated using the method in SI Text 7. HCE gives a measure of the fouling that is reversed by the hydraulic backwashing process²⁸, while HIFI is a measure of fouling that is not reversed by either hydraulic backwashing or the photocatalytic processes taking place on the membrane surface^{21, 28}.

Following a previously developed method on a Metawater ceramic membrane monolith pilot plant fed with secondary treated waste water⁴, the reduced chemical consumption of the photocatalytic membrane system can be determined by a calculation of the time to a chemical clean when TMP reaches a certain threshold, which would trigger a clean-in-place (CIP) event in a real plant. This is the time taken for TMP to reach 150 kPa, representing the average maximum pressure rating of the dead-end filtration feed pump used in the reported pilot plant

trial. The time to chemical clean was calculated by plotting the TMP values just after each backwashing event against time, then calculating the time needed to reach 150 kPa through linear regression and extrapolation to this target threshold pressure.

The reduced pump energy consumption of the solar-activated membrane was also compared to the pump energy consumption during filtration without solar activation. The specific electrical energy consumption of the pump, E (kWh/m³) calculated according to the method described in SI Text S3, was used to compare different operating modes.

2.4. Quantification of hydroxyl radicals

The concentration of hydroxyl radicals produced by the photocatalytic membranes in the different configurations was determined indirectly by using para-chlorobenzoic acid (*p*CBA) as a probe compound. The experimental method is given in SI Text S4.

2.5. Water samples analysis

Total organic carbon (TOC) for the water samples was measured by a Sievers M5310C Laboratory TOC Analyser. The conductivity of water samples was measured using an Orion Versastar Pro Advanced Electrochemistry Meter from Thermo Scientific. The turbidity of water samples was measured by a HACH 2100N Turbidimeter. The turbidity is reported in accordance with the United States Environmental Protection Agency (EPA) Method 180.1³¹,³². Colour and specific UV absorption at 254 nm (UV₂₅₄) were measured by a HACH DR5000 spectrophotometer.

2.6. Carbon concentration measurements and mass balance calculations

Carbon concentrations were determined from TOC data. Each sample was first filtered through a 0.45 μm disposable syringe filter prior to injection to prevent clogging of the TOC analyser. A series of equations were applied to determine, by mass balance, the percentage of carbon that was retained on the membrane, and whether the carbon was retained reversibly or irreversibly. These carbon mass balance equations are given in the Supplementary Information (SI) (Equations S6-S15).

2.7. Size exclusion chromatography

An Agilent Technologies 1200 HPLC with a SEC column, a fluorescence detector (FLD), a diode array detector (DAD) and a Sievers M9 Portable TOC Analyser was used to analyse the fraction of organics in water before and after filtration events. The analytical method was adopted from previous work ³³, and briefly described in SI Text S5. A DAD was used to measure absorbance at a fixed wavelength of 254 nm to characterise DOM chromophores as a function of AMW ²⁶. The method for determination of AMW is given in the SI Text S6. Fluorescence was used for the detection of Peak C fluorescent compounds at excitation wavelength of 350 nm and an emission wavelength of 450 nm. Peak C fluorescence refers to the NOM fluorescence signal that occurs in the excitation range of 320-365nm, and emission range of 420-470nm. It has been found to commonly occur across a diverse range of NOM samples from aquatic environments, and is related to the presence of humic substances (in both fresh and marine water samples) ³⁴ and protein-like fluorophores ³⁵.

3. Results and discussion

3.1. Membrane substrate optical properties

Figure 1 (a) presents the transmittance of light coming from the solar simulator, through the quartz window fixed in the membrane module as well as the porous glass membrane substrate. The spectral irradiance of the solar simulator, emitting at 23% of full capacity, (equivalent to 0.35 Suns), is shown in Figure 1 (b). These experiments therefore utilize irradiance levels similar to sunlight indirectly shining into the module window. The quartz window is highly transparent (>80%) to UV light in the measured spectral range. The sintered glass substrate is largely as transparent as the quartz window in the shorter wavelengths below 355 nm but drops to around 10% above 370 nm. This is sufficient for purposes of this study because wavelengths below 385 nm (3.2 eV) correspond to the band gap energy of the anatase phase in Degussa P25 TiO₂^{37,38}. Photocatalyst activation requires energy equal to or greater than the band gap energy, therefore the higher transparency of the sintered porous glass substrates in the range of 340 – 355 nm (3.6 – 3.5 eV) is desirable. However, the irradiance measured through the porous glass (that would be delivered to the photocatalyst coating) was highest for the longer wavelengths (Figure 1 b), due to the increased output of the solar simulator at higher wavelengths. This is consistent with the spectrum of solar radiation, which is 4-5% UV and more than 90% visible light and infrared radiation³⁹. This is the key novelty for the work presented here, where the enabling feature of this new membrane concept using natural sunlight to reduce chemical use, needs to be demonstrated.

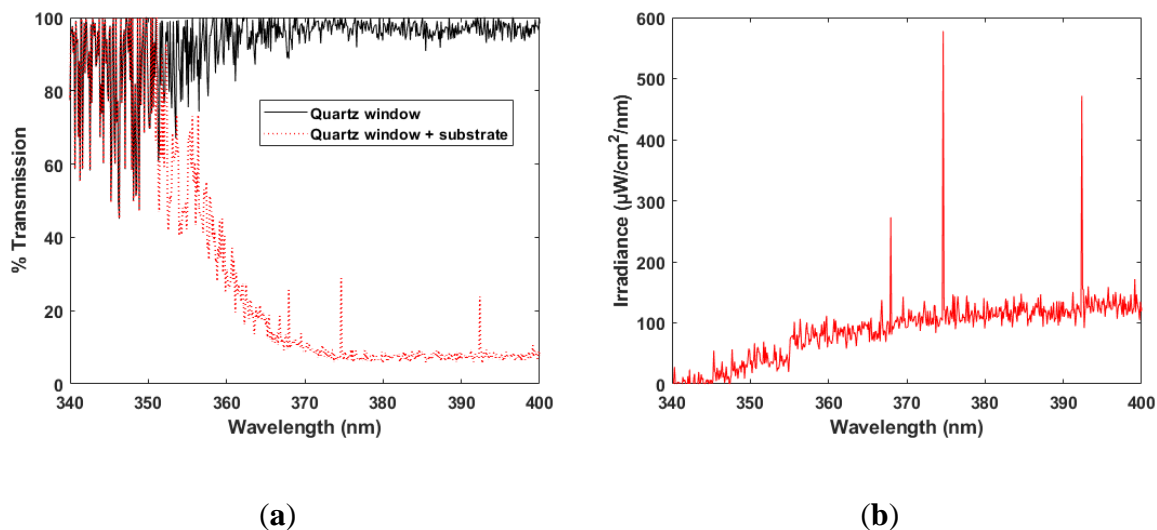


Figure 1. The transmittance of the quartz window and sintered porous glass membrane to indirect light (0.35 suns) from the solar simulator (a) and the spectral irradiance of light through the quartz window and wet porous glass substrate, being the light expected to arrive at the membrane's photocatalytic layer (b).

3.2. Membrane fouling during surface water filtration

Figure 2 shows the normalised pressure-time profiles of the TiO₂ coated membrane without solar irradiation (C-OFF) and under partial (0.35 suns) solar radiation (C-ON). A high TMP rise during filtration without solar irradiation occurred compared to when solar irradiation was present. Just before backwashing, the maximum TMP without solar irradiation was at least 2-fold more than the corresponding TMP with solar irradiation. The beneficial effects of solar irradiation are reflected in the HIFI values of 0.0001 m²/L and 0.0008 m²/L with and without irradiation, respectively. The 8-fold reduction in HIFI confirms the sunlight's effectiveness to minimise the irreversible fouling of the membrane. These HIFI values show better values from previously reported work on bovine serum albumin (BSA) filtration with the same membrane, where the HIFI was 3-fold lower with UV-LED irradiation²¹. Moreover, the BSA solution

TOC concentration was about half compared to TOC of the water samples used in the current work (Table 3). In comparing our HIFI to prior work, others reported much higher values, for example $0.0297 \text{ m}^2/\text{L}$ obtained from surface water filtration with a commercial single channel tubular ceramic membrane with $0.20 \mu\text{m}$ sized pores,⁴⁰ and $0.0023 \text{ m}^2/\text{L}$ obtained for utility raw water filtration with a hollow fibre polyvinylidene fluoride (PVDF) membrane with $0.05 \mu\text{m}$ sized pores⁴¹. The significant reduction in filtration resistance was attributed to the already higher hydrophilicity of TiO_2 ⁴² (without light), then due further to induced surface superhydrophilicity upon solar irradiation, seen by others through a reduction in the water contact angle⁴³.

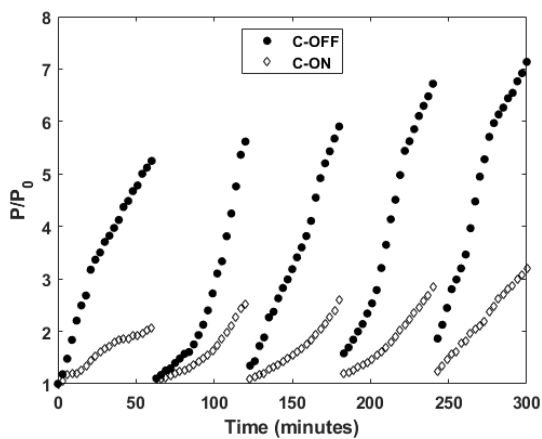


Figure 2. Normalised pressure-time profiles for the filtration of surface water of the TiO_2 coated glass membrane in dark (C-OFF) and with 0.35 suns simulated sunlight (C-ON) with periodic (hourly) backwash at an operating flux of $300 \text{ L}/\text{m}^2/\text{h}$ and temperature of 24°C . P is the TMP at the selected time interval and P_0 ($12.0 \pm 2.0 \text{ kPa}$) is the initial TMP.

Both operating conditions showed high hydraulic cleaning efficiency (HCE) values of the membrane in both instances when solar irradiation was provided ($95 \pm 2\%$) and when it was not

(95±1%). These values are comparable to those we previously obtained for BSA filtration with UV light emitting diode (LED) irradiation (92±2% and 96±2%, respectively)²¹, and could be attributed to the already known hydrophilic property of TiO₂.

Time to chemical clean (TtCC) was used to further investigate which aspect of filtration was improved with solar irradiation. TtCC values, calculated from the method described in Section 2.3, are shown in Table 1. With solar irradiation TtCC was 8.8 days, compared to just 2.0 days without solar irradiation. Chemical cleaning on a real plant, for example with chemically enhanced backwashes (CEBs), are often adopted on daily to weekly basis to maintain low TMP over longer periods before shutting down the plant for an intensive CIP. In our case, solar irradiation has postponed any use of chemicals (CEB or CIP) by 4.5-fold using this measure. To postpone chemical cleaning even longer, the photocatalytic membrane in this study could be operated at a lower flux but would need further testing to verify in the given context of feed water properties and practical access to cleaning chemicals. Also, since sunlight availability is limited by time of day and weather, further work would be needed to develop operational routine for the specific context (e.g., filtering 24 h a day and using sunlight when available to offset chemicals versus filtering only when sunlight available).

The improvement from sunlight application was also quantified in terms of filtration energy saving. As shown in Table 1, when the energy consumed by the pump alone for filtration is considered (Equation S2), the solar activated TiO₂ coated membrane had an energy consumption of 0.01 kWh/m³ compared to 0.02 kWh/m³ when it was not irradiated with solar radiation. The values do not take into account other energy consuming components such as backwashing and air compressors, since the setup used manual backwashing. As a reference to the calculated values, the energy consumption compares closely to previously reported values for practical MF systems in the range of 0.09-0.1 kWh/m³⁴⁴, although these have considered the full MF process energy requirements. Backwashing may be the additional contributor to

MF plant electrical energy required, which should be in turn lower with a less fouled membrane. The reduced energy from solar cleaning is therefore indicative of the potential for overall plant reduced electrical energy consumption.

Table 1. Operating flux, time to chemical clean (TtCC) and pump electricity demand values of the coated membrane without and with solar radiation.

Solar Status	Flux (L/m²/h)	TtCC (days)	Pump electricity demand (kWh/m³)
C-OFF	300	2.0	0.2
C-ON	300	8.8	0.1

3.3. Hydroxyl radical analysis to confirm photocatalytic effect

The calculated concentrations and rate of production of hydroxyl radicals are shown in Figure 3 (a) and Figure 3 (b) respectively. Because the method of quantification of hydroxyl radicals is an indirect method, which actually measures the removal of *p*CBA, some amount of radicals is shown to have been formed for configurations where the conditions were not suitable for photo-induced hydroxyl radical formation (i.e. dark conditions). These are abbreviated C-OFF (coated membrane-light off) when the membrane is not illuminated with light and B-OFF (bare membrane-light off) when the uncoated substrate is not illuminated. Apparent hydroxyl radical concentration based on *p*CBA concentration reduction by the coated membrane without solar irradiation is 1.0×10^{-15} M. The apparent radical formation in these instances could be due to adsorption of *p*CBA onto the membrane surface, or physical rejection. It has been shown in previous studies that some adsorption on photocatalyst and substrate surfaces occurs prior to

photocatalytic oxidation^{45,46}. The non-illuminated experiments serve as controls to determine the extent of *p*CBA reduction due to non-photocatalytic processes. Radical formation would be expected on the illuminated coated membrane (C-ON) due to the photocatalytically active TiO₂. Previous studies found that *p*CBA degradation through direct photolysis proceeds slowly compared to the advanced oxidation degradation pathway⁴⁷. Observed *p*CBA degradation would therefore be expected to be a result of photocatalysis rather than photolysis. When the experimental controls have been taken into consideration (light off and absence of photocatalyst), the steady state concentration of hydroxyl radicals produced by the membrane through the photocatalytic process in the presence of light is 3.5×10^{-15} M (determined by subtracting the control concentration from the observed hydroxyl concentration during C-ON conditions). Figure 3 (b) also shows a 3-fold higher rate of production of radicals from the TiO₂ surface under illuminated conditions compared to dark conditions. Steady concentrations of hydroxyl radicals were achieved after about 30 minutes of filtration. In comparison, these steady state concentrations of hydroxyl radicals are an order of magnitude lower compared to other advanced oxidation systems ranging from 3.1×10^{-14} M to 1.0×10^{-13} M. At these concentrations, hydroxyl radicals were capable of inactivating adenovirus (4 log)³⁰, transforming aliphatic, aromatic and olefinic DOM moieties¹⁷ and degrading *p*CBA in water matrix low-carbon tap water and well water⁴⁸. With further optimisation in the current setup (such as using custom fabricated transparent porous glass and/or means to better direct light to membrane window), it may be possible to achieve these prior reported radical concentrations. However, the result still addressed our primary aim which was to confirm OH radical formation when partial sunlight is distributed to the photocatalyst via the porous glass substrate, and thus allows us to conclude that photocatalytic activity is indeed present, and produced OH radicals are sufficient in production to greatly assist with membrane cleaning.

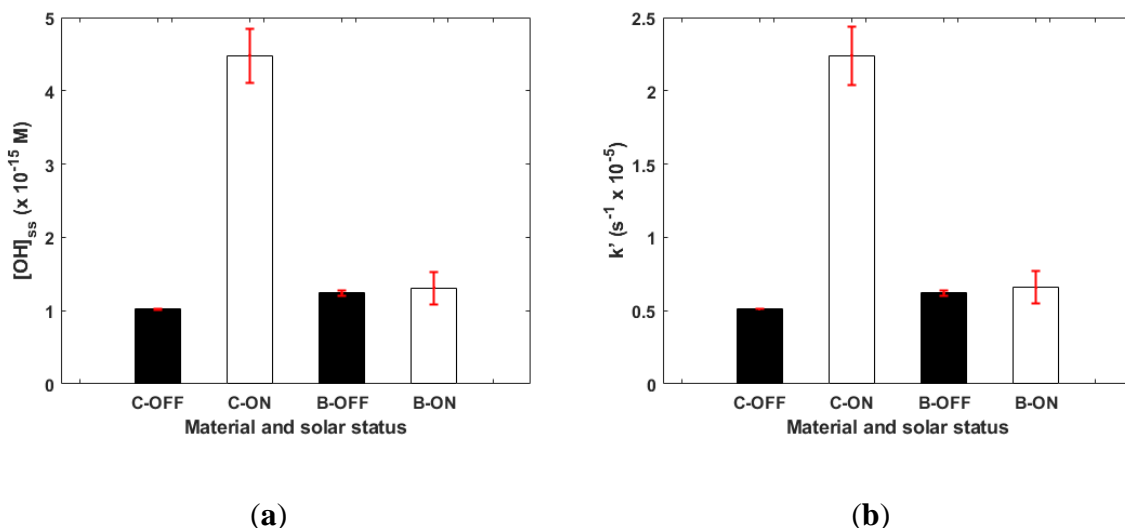


Figure 3. Steady state concentration of generated hydroxyl radicals (a) and the pseudo first order reaction rate (b). These were obtained using a 0.6 mg/L solution of *p*CBAs as a probe compound at a flux of 300 L/m²/h and room temperature. The abbreviations stand for coated membrane-light OFF (C-OFF), coated membrane-light ON (C-ON), bare membrane light OFF (B-OFF) and bare membrane light ON (B-ON).

3.4. Evaluation of water quality

The water samples were analysed for turbidity, specific UV absorbance at 254 nm and TOC as well as characterisation through HPSEC.

3.4.1. Turbidity and UV254

Table 2 shows the turbidity and UV254 values of the various water samples. The TiO₂ coated membrane removed at least 94% turbidity in permeate compared to 39% for the bare substrate. All the backwash samples had more turbidity than their respective permeate samples, but the backwash turbidity in all cases (except B-OFF which was similar) were never higher than the initial (feed) where an increase may be expected. This may be due to compaction of the solids

due to filtration. In terms of UV254, this measure correlates to the aromatic content of the organic molecules present in the feed water ⁴⁹. The coated membrane reduced UV254 absorbance by 26%, being higher than at least 3% reduction for the bare substrate, which is understandable considering the pore size of the coarse filter of 1.5 μm used to pre-treat the samples prior to storage was similar to the bare substrate. Meanwhile, backwash UV254 absorbance increased uniquely for the coated membrane compared to the permeate used to produce the backwash, indicating the return to solution of the rejected soluble organics because of backwashing, as detected by this method.

However, these results are mostly showing the basic filtration differences between the coated and uncoated membranes. No appreciable differences to the samples could be seen as a result of solar irradiation (ON vs OFF). This is a unique finding, since photocatalytic effects on the bulk solution organics is often first observed by a decline in UV254 light absorbance ⁴. Deeper analysis into the water quality will now be considered to assess how the light assisted with reduced TMP rise as observed in Figure 2.

Table 2. Turbidity and UV254 values of sampled and filtered water. Error ranges are the standard error calculated from experimental data

Membrane	Initial Turbidity (NTU)	Permeate Turbidity (NTU)	Backwash Turbidity (NTU)	Initial UV254 (A.U)	Permeate UV254 (A.U)	Backwash UV254 (A.U)
C-OFF	3.2 \pm 0.1	0.20 \pm 0.01	0.80 \pm 0.01	0.090	0.064 \pm 0.001	0.093 \pm 0.001
C-ON	3.3 \pm 0.1	0.15 \pm 0.01	1.0 \pm 0.1	0.090	0.067 \pm 0.001	0.087 \pm 0.001
B-OFF	3.3 \pm 0.1	2.1 \pm 0.1	3.4 \pm 0.1	0.091	0.084 \pm 0.003	0.086 \pm 0.001
B-ON	3.3 \pm 0.2	2.0 \pm 0.1	2.3 \pm 0.02	0.091	0.088 \pm 0.002	0.088 \pm 0.001

3.4.2. Total organic carbon rejection

Table 3 shows the TOC values of the feed, permeate and backwash for the coated and bare membranes, with and without solar irradiation. Generally, similar behaviour can be seen in terms of rejection and some return to solution in the backwash as was observed through turbidity and UV254 absorbance in Table 2, with slight changes associated with solar irradiation observed from the concentration values.

Looking more closely at TOC, using the carbon mass balance equations (Equations S6-S15), the percentage of carbon removed by the membrane shown in Figure 4 (a), and the carbon contribution to both reversible and irreversible fouling shown in Figure 4 (b) were calculated. The membrane removed 24% of the carbon from the feed, with the amount rising to 30% with solar irradiation. The removal values are statistically different as determined by a student's paired t-Test ($p = 0.8$). It appears that modification of the substrate with TiO_2 helped to improve the hydrophilicity of the surface, which helps in rejecting hydrophobic foulants arriving at the membrane surface. The bare uncoated substrate rejected only 9% of carbon whether there was solar irradiation or not. This was due to the substrate's larger mean pore size of $1.4 \mu\text{m}$ compared to $0.53 \mu\text{m}$ for the coated membrane, as previously reported ²¹. In addition, as mentioned previously, the coarse filter used to pre-treat the samples had a similar pore size of $1.5 \mu\text{m}$.

Retained carbon attributed to lost/irreversible/undissolved carbon (M_{IL}) carbon was largest for the bare substrate, accounting for more than $0.93 \text{ mg C/mg } C_{\text{F}}$ (mg of carbon per mg of carbon fed to the membrane) of retained carbon type, as shown in Figure 4 (b). The importance of solar irradiation and subsequent photocatalysis in increasing carbon that can be recovered after retention (and indicate reduced carbon material fouling) can be seen for the TiO_2 coated membrane. Even though in both instances the coated membrane had higher carbon removal than the bare membrane, without solar irradiation, the normalised lost carbon (M_{IL}) was 0.93

mg C/mg C_F, decreasing to 0.73 mgC/mgC_F with solar irradiation. Lost carbon is the sum of carbon retained irreversibly on the membrane and that which did not redissolve, and recovered carbon makes up the redissolved part of reversible carbon fouling, thus the values give an indication of the extent of irreversible carbon fouling.

Table 3. TOC values of sampled and filtered water. Error ranges are the standard error calculated from experimental data.

Membrane	Initial TOC (mg/L)	Permeate TOC (mg/L)	Backwash TOC (mg/L)
C-OFF	13.9±0.1	10.5±0.1	11.0±0.1
C-ON	13.9±0.1	9.8±0.1	14.6±0.1
B-OFF	13.8±0.1	12.6±0.2	12.7±0.2
B-ON	13.9±0.1	12.6±0.2	12.8±0.2

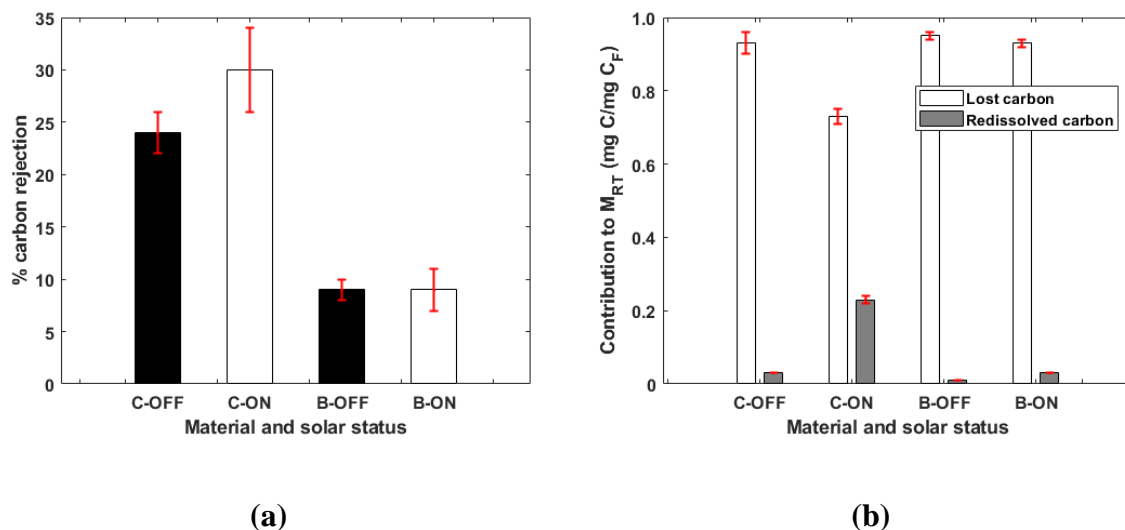


Figure 4. TOC rejection (a) and the contribution of redissolved reversible carbon (M_{RR}) and lost/irreversible/undissolved carbon (M_{IL}) to total retained carbon (M_{RT}), normalised to the amount of carbon fed to the membrane (b). $p = 0.8$, calculated through Student's paired t-Test, with a two-tailed distribution.

3.5. High performance size exclusion chromatography (HPSEC)

The components of the water samples were separated by the column into two main fractions, as presented in Table 4. From literature, Fraction I (33-5 kDa) consists of biopolymers and Fraction II (5-0.4 kDa) consists of humic substances and building blocks³⁶.

Table 4. Fractions of organics separated by the HPSEC column according to their apparent molecular weight (AMW)

Fraction	Maximum AMW (kDa)	Minimum AMW (kDa)	Elution time (minutes)
I	33	5	20 – 33
II	5	0.4	33 – 49

3.5.1. HPSEC-TOC

The HPSEC-TOC results of water samples run with the TiO₂ coated (C) and uncoated (B) membrane, with and without solar radiation (ON and OFF) are shown in Figure 5. The coated membrane with smaller pore size had significant TOC rejection (~80%) compared to the bare substrate (~0%) (Figure S2), and there was a progressive decrease in the percentage TOC rejection from the larger Fraction I (Light off = 86%, Light on = 76%) to the smaller Fraction II (Light off = 77%, Light on = 72%) due to size-controlled retention on the membrane surface. The backwashes also had relatively lower TOC values because as concluded earlier from compaction, some carbon was in particle form (visible from experiment) and did not redissolve and was removed by the 0.45 μm sample filtration in the TOC method.

From the results of C-OFF, the molecular weight cut off (MWCO) of the membrane was determined to be 21 kDa. This corresponds to a mean pore size of ~0.5 μm⁵⁰, which is agreement with the pore size we previously obtained through porometry²¹ classifying the coated membrane in the MF range often used for water filtration^{51, 52}. Improved substrates, smaller pore size and thinner membranes could be developed in future work, where the same light conducting glass substrate concept could be enhanced with improved transmittance and/or extended other applications such as photocatalytic coatings on ultrafiltration (UF) membranes [11, 14].

The results showing minimal change to MW profile of the TOC indicate that the benefit of photocatalysis in the current process is not associated to changes in bulk solution organics. Changes in hydrophobicity of the DOM, as seen in previous studies¹⁷, could also have contributed to reduced fouling. In a previous study, it was established that even though transformation of DOM by hydroxyl radicals occurs, it does not translate to significant

dissolved organic carbon (DOC) removal¹⁷. Instead, DOM structures are transformed to lower molecular weight organic compounds such as ketones, alcohols, carboxylic acids and final products such as formic acids, acetic acids and oxalic acids.⁵³ It is possible to pick up these transformations using spectral indices such as UV254 and fluorescence, but a comprehensive identification would require mass spectrometry⁵⁴. Our results confirm that membrane rejection is the primary cause of less TOC in permeate, rather than any effect from solar irradiation (and in turn photocatalysis). Instead, there appears to be a harder to measure altered organic-membrane surface chemistry interaction that assists reducing fouling.

Looking at the backwash C-ON profile shown in Figure 5b, it displays a shift in AMW distribution compared to the C-OFF profile. The C-OFF profile contains a shoulder near the high AMW end of the Fraction II region (elution time ~38 minutes) while the C-ON profile contains a shoulder peak near the low AMW end of the Fraction II region (elution time ~45 minutes). This suggests the transformation of DOM molecules from higher to lower AMW, induced by photooxidation in the presence of solar radiation. Unlike the permeated DOM which showed little change from solar irradiation, the DOM caught at the membrane surface are continuously exposed to photooxidative processes, leading to reaction and observable transformations.

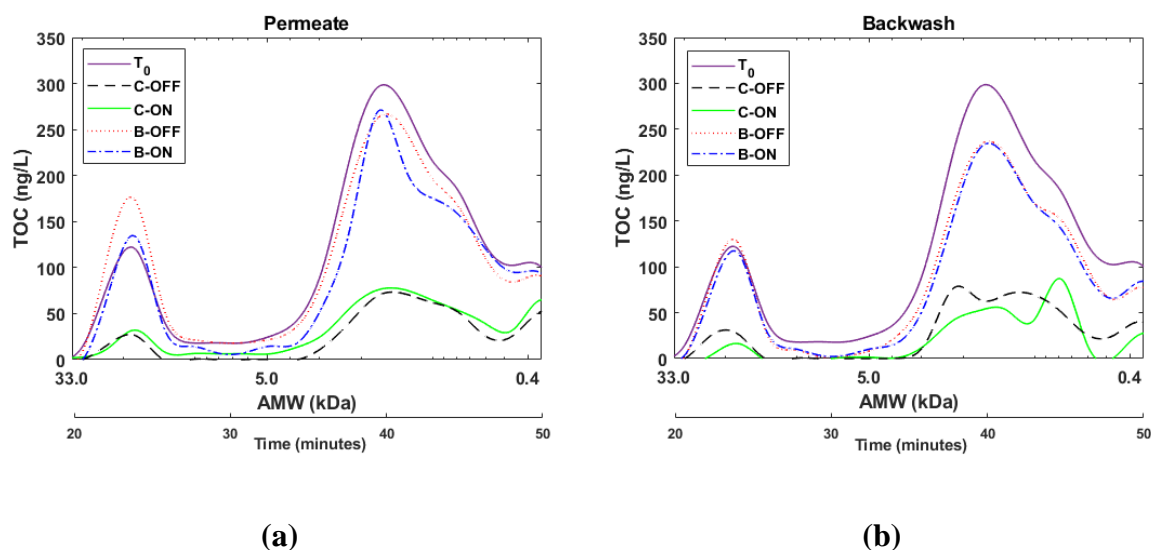
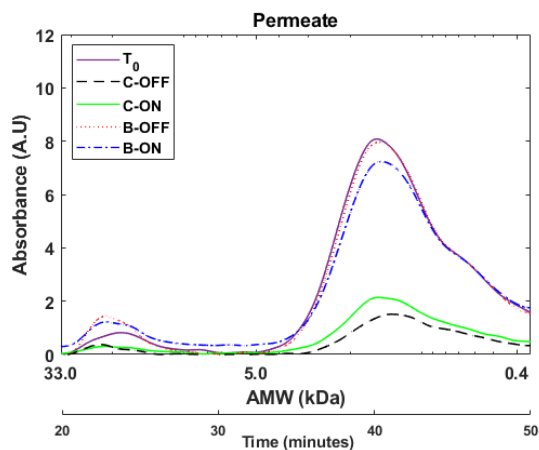


Figure 5. HPSEC-TOC chromatograms of permeate (a) and collected backwash fraction (b). T_0 refers to signal from the feed.

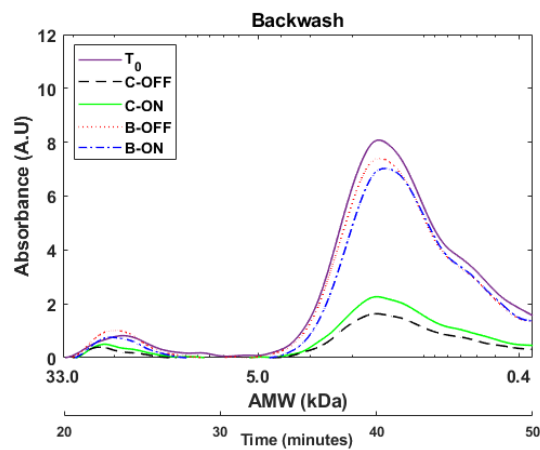
3.5.2. HPSEC-fluorescence and UV254 detection

The absorbance and fluorescence profiles of the water samples are shown in Figure 6. Fluorescence peaked at 1.4 kDa, with the feed solution profile dropping little in magnitude for the uncoated membrane permeate, but dropped substantially for the coated membrane permeate while maintaining a similar profile shape (i.e. peak still at 1.4 kDa). Solar irradiation had little influence on the permeate fluorescence profile shape and magnitude. Like the prior observations on organics, this is an indication that rejection, rather than oxidation, was the likely cause of the decreased fluorescence in permeate. This means that solar irradiation had no influence in the materials detected by fluorescence, used to measure the rejection of the fluorescent, non-biopolymer fractions of the water samples, in particular humic-like substances (Fraction II), which emit and absorb at the selected excitation (350 nm) and emission wavelengths (450 nm)³⁶.

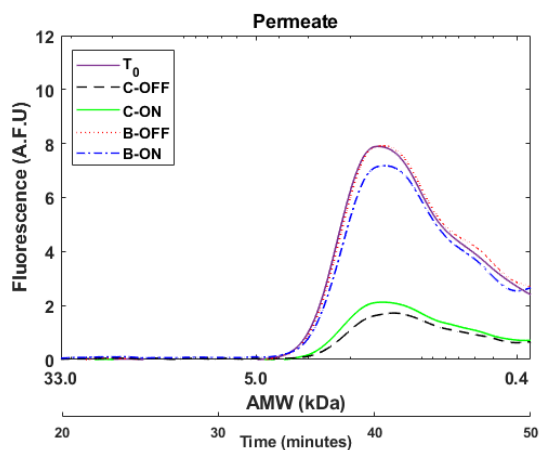
Like fluorescence, there was no clear shift in MW observed in the UV254 absorbance profiles. The fact that a shift is only seen in the TOC backwash profile (and not the UV254 and fluorescence backwash profiles) suggests that transformations occurred with molecules that are not optically active (do not absorb or fluoresce light, i.e., likely less aromatic and more aliphatic in nature). However, there is a slight increase in the UV254 absorbance for the permeate with solar irradiation, implying there may be an effect to enhance diffusion of molecules in Fraction II.



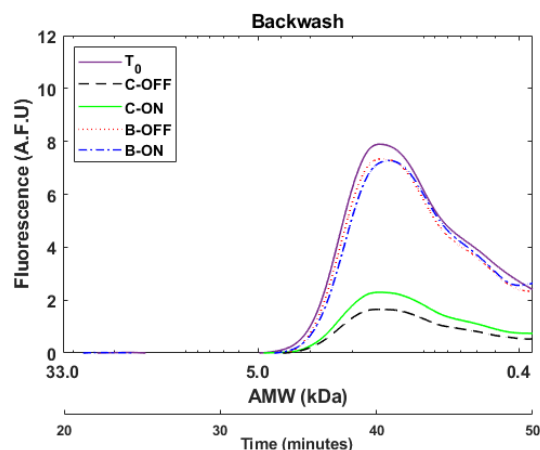
(a)



(b)



(c)



(d)

Figure 6. HPSEC-UV254 chromatograms of permeate (a) and collected backwash fraction (b) as well as HPSEC-Fluorescence chromatograms of permeate (c) and collected backwash fraction (d). The abbreviations stand for coated membrane-light OFF (C-OFF), coated membrane-light ON (C-ON), bare membrane light OFF (B-OFF) and bare membrane light ON (B-ON). T_0 refers to signal from the feed.

3.6. Assessment of behaviour of organic fractions to rejection, fouling, and diffusion through the membrane

Through HPSEC, the coated membrane was found to be in the MF category and also revealed humics may be facilitated to permeate the membrane due to light activation related to their varying degrees of heterogeneity, with both hydrophobicity and hydrophilicity occurring in these compounds ⁴⁹, coupled with a proposed increased membrane hydrophilicity. However more significantly, a shift to lower MW was observed on the TOC backwash profile under solar radiation, where organics were exposed to reactions for longer times and therefore transformations were more measurable and demonstrated reduced organics adhesion to the membrane surface from solar irradiation.

This transformation can occur by advanced oxidation on the surface, confirmed by measurement of hydroxyl radicals being a quantitative contribution of the radical to the reaction rates with DOM ¹⁷. DOM is a complex mixture of compounds with different reactivities to HO[•], but the overall reaction rate constant for the reaction of HO[•] with DOM has been experimentally determined to be $k = (1.39-4.53) \times 10^8 \text{ M}^{-1} \text{ s}^{-1} \text{ DOM}^{17}$. Complete transformation of DOM would require hydroxyl radical reaction with other targeted groups such as oxalate, formate and acetate. For example, the rate constant for HO[•] reaction with oxalate is reported to be $4.7 \times 10^7 \text{ M}^{-1} \text{ s}^{-1}$, with acetate it is $7.3 \times 10^7 \text{ M}^{-1} \text{ s}^{-1}$, and with formate groups is $3.2 \times 10^9 \text{ M}^{-1} \text{ s}^{-1}$ ¹⁷. This shows that the transformation of organic carbon that continuously arrives at the membrane surface is not straightforward but also dependent on many different reactions with different rate constants and intermediates. Moreover, the estimated contact time of 80 ms (calculated from Equation S16) would not allow significant DOM transformation at the measured concentration of generated hydroxyl radicals and rate constant. Such transformations would require more contact time or increased hydroxyl radical generation through a combination of measures such as multiple pass filtration, reduced flux,

increased thickness of TiO₂ layer and more solar radiation arriving at the TiO₂ layer. In previous work, through light ON and OFF cycles, we were able to demonstrate that anti-fouling conditions were only maintained when light was ON, confirming the importance of photocatalysis in the membrane operation ²¹.

Using the results from this study, the overall effect to the beneficial performance of the membrane is represented graphically by the mechanisms in Figure 7. This includes representation as a practical setup within an inside-out dead-end filtration system that is typical of current commercial ceramic membrane monoliths. Combined effects of surface photocatalysis and enhanced hydrophilicity greatly reduces resistance during filtration as water molecules dominate the foulant-membrane interface, and increase regular backwash efficiency with minimised irreversible fouling. Water would especially work as a good solvent for washing off hydrophilic components.

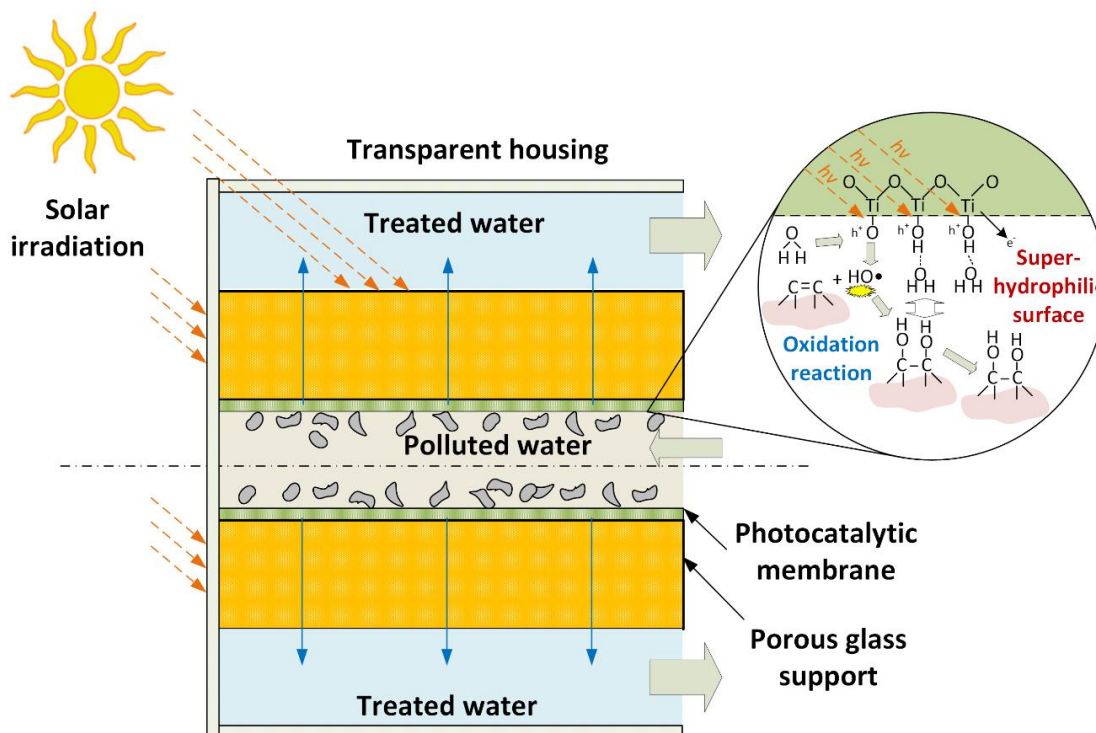


Figure 7. Visual representation of a concept solar irradiated porous glass monolith channel coated with photocatalytic membrane within a transparent side and end housing. Expanded view of membrane surface shows the beneficial effects of receiving light via the glass substrate to the photocatalyst membrane surface, which include changes to surface chemistry and attack of organic compounds by hydroxyl radicals.

While the novelty of this work focussed on demonstrating the viability for solar cleaned membranes to filter non-potable water using the innovative light transmitting substrates, several effects could be further explored to not only understand and confirm the dominant positive effects such as light-stimulated hydrophilicity observed by others as compared to organic-membrane surface oxidations, but also the possibility for even more beneficial effects. Stability of the TiO_2 may be of concern, but the P25 material is known to have high stability

to typical surface water properties⁵⁶. In our own work, the thickness of the TiO₂ coating of about 15 µm was preserved as shown in SEM images at the conclusion of experimental work²¹, indicating no significant loss of the coating. In terms of more valuable features of this technology, the novel photocatalytic membrane may lead to favourable reactions on the particles attached to the membrane surface, such as disinfection of pathogens that are rejected in the backwash and understanding anti-fouling behaviour with varying proportions of hydrophobic and hydrophilic organic fractions. Further work to explore these and more effects is warranted. The sustainability of cleaning cycles triggered with sunlight availability would also be a good next step in the development of the membrane system.

4. Conclusions

This work successfully demonstrated the potential for reduced chemical and energy consumption in membrane water treatment by adopting solar-activated photocatalysis in a light-transmitting membrane. The specific findings from this work were:

- Even though transmission light through the membrane substrate was about 10% on average, it was sufficient to facilitate production of a photocatalytic response on the membrane surface;
- Photocatalytic activation resulted in significant reduction in filtration resistance and 8-fold reduction in irreversible fouling, leading to halving of pump energy consumption during filtration. More importantly, a potential for reducing the frequency of time to CIP from 3 months to more than a year was demonstrated. This time to CIP frequency reduction could be achieved by simply exposing the photocatalytic membrane to the sun, without any CEBs during the entire operation;

- The membrane has potential for adoption in remote communities where use of chemicals in water treatment is a challenge, whereby sunlight helps to maintain the functionality of the membrane and producing clean water for the community; and
- Further work is justified to precisely identify the demonstrated antifouling effects, correlated in this work to two key effects, 1 – oxidation of surface attached organic foulants confirmed in our work to be likely by hydroxyl measurements, and 2 – superhydrophilicity activated by photocatalysis reported by others. These could lead to discovery of more useful features such as in-situ disinfection of surface-attached pathogens and antifouling/separation behaviour as a function of the fraction of hydrophobic to hydrophilic organics.

Supporting Information

This material is available free of charge via the internet at <http://pubs.acs.org>.

Chemicals used in the experiments (Text S1), filtration setup (Text S2), schematic representation of the filtration system (Figure S1), pump power demand (Text S3), quantification of hydroxyl radicals (Text S4), size exclusion chromatography method (Text S5), apparent molecular weight calibration method (Text S6), fouling indices calculations (Text S7), carbon mass balance equations (Text S8), contact time calculation (Text S9), rejection percentage based on HPSEC (Text S10 and Figure S2), and HPSEC chromatograms of permeate and collected backwash fractions (Figure S3).

Acknowledgements

The Victoria University International Postgraduate Scholarships (VUIPRS) and the Institute for Sustainable Industries and Liveable Cities (ISILC) at Victoria University, Melbourne supported this work through invaluable funding. ISILC and the Mortenson Center in Global Engineering at the University of Colorado (CU), Boulder, USA, also provided funds to make possible the research visit to the Sustainability, Energy and Environment Laboratory (SEEL) at CU where this work was carried out. We would also like to acknowledge Dr. Frank Leresche, Bryan Liu, Jasmine Gamboa and Dr. Sarah Fischer, members of SEEL who were always available to lend assistance with laboratory instrumental analysis despite their own busy schedules.

References

1. Bhojwani, S.; Topolski, K.; Mukherjee, R.; Sengupta, D.; El-Halwagi, M. M., Technology review and data analysis for cost assessment of water treatment systems. *Science of The Total Environment* **2019**, *651*, 2749-2761.
2. Madaeni, S. S.; Ghaemi, N., Characterization of self-cleaning RO membranes coated with TiO₂ particles under UV irradiation. *Journal of Membrane Science* **2007**, *303* (1–2), 221-233.
3. Zhang, W.; Ding, L.; Luo, J.; Jaffrin, M. Y.; Tang, B., Membrane fouling in photocatalytic membrane reactors (PMRs) for water and wastewater treatment: A critical review. *Chemical Engineering Journal* **2016**, *302*, 446-458.
4. Dow, N.; Murphy, D.; Clement, J.; Duke, M. *Outcomes of the Australian Ozone/Ceramic Membrane Trial on Secondary Effluent*; AWA Water: 2013; pp 45-51.
5. Athanasekou, C. P.; Moustakas, N. G.; Morales-Torres, S.; Pastrana-Martínez, L. M.; Figueiredo, J. L.; Faria, J. L.; Silva, A. M. T.; Dona-Rodríguez, J. M.; Romanos, G. E.; Falaras, P., Ceramic photocatalytic membranes for water filtration under UV and visible light. *Applied Catalysis B: Environmental* **2015**, *178*, 12-19.
6. Vanangamudi, A.; Dumée, L. F.; Ligneris, E. D.; Duke, M.; Yang, X., Thermo-responsive nanofibrous composite membranes for efficient self-cleaning of protein foulants. *Journal of Membrane Science* **2019**, *574*, 309-317.
7. Vanangamudi, A.; Saeki, D.; Dumée, L. F.; Duke, M.; Vasiljevic, T.; Matsuyama, H.; Yang, X., Surface-Engineered Biocatalytic Composite Membranes for Reduced Protein Fouling and Self-Cleaning. *ACS Applied Materials & Interfaces* **2018**, *10* (32), 27477-27487.
8. Ngo, T. H. A.; Nguyen, D. T.; Do, K. D.; Minh Nguyen, T. T.; Mori, S.; Tran, D. T., Surface modification of polyamide thin film composite membrane by coating of titanium dioxide nanoparticles. *Journal of Science: Advanced Materials and Devices* **2016**, *1* (4), 468-475.

9. Rabiee, H.; Farahani, M. H. D. A.; Vatanpour, V., Preparation and characterization of emulsion poly(vinyl chloride) (EPVC)/TiO₂ nanocomposite ultrafiltration membrane. *Journal of Membrane Science* **2014**, *472*, 185-193.
10. Qian, Y.; Chi, L.; Zhou, W.; Yu, Z.; Zhang, Z.; Zhang, Z.; Jiang, Z., Fabrication of TiO₂-modified polytetrafluoroethylene ultrafiltration membranes via plasma-enhanced surface graft pretreatment. *Applied Surface Science* **2016**, *360*, 749-757.
11. Geng, Z.; Yang, X.; Boo, C.; Zhu, S.; Lu, Y.; Fan, W.; Huo, M.; Elimelech, M.; Yang, X., Self-cleaning anti-fouling hybrid ultrafiltration membranes via side chain grafting of poly(aryl ether sulfone) and titanium dioxide. *Journal of Membrane Science* **2017**, *529*, 1-10.
12. Banerjee, S.; Dionysiou, D. D.; Pillai, S. C., Self-cleaning applications of TiO₂ by photo-induced hydrophilicity and photocatalysis. *Applied Catalysis B: Environmental* **2015**, *176–177*, 396-428.
13. Chen, J.; Poon, C.-s., Photocatalytic construction and building materials: From fundamentals to applications. *Building and Environment* **2009**, *44* (9), 1899-1906.
14. Madaeni, S. S.; Ghaemi, N.; Alizadeh, A.; Joshaghani, M., Influence of photo-induced superhydrophilicity of titanium dioxide nanoparticles on the anti-fouling performance of ultrafiltration membranes. *Applied Surface Science* **2011**, *257* (14), 6175-6180.
15. Buck, C.; Skillen, N.; Robertson, J.; Robertson, P. K. J., Photocatalytic OH radical formation and quantification over TiO₂ P25: Producing a robust and optimised screening method. *Chinese Chemical Letters* **2018**, *29* (6), 773-777.
16. Zhang, J.; Nosaka, Y., Generation of OH radicals and oxidation mechanism in photocatalysis of WO₃ and BiVO₄ powders. *Journal of Photochemistry and Photobiology A: Chemistry* **2015**, *303-304*, 53-58.
17. Varanasi, L.; Coscarelli, E.; Khaksari, M.; Mazzoleni, L. R.; Minakata, D., Transformations of dissolved organic matter induced by UV photolysis, Hydroxyl radicals, chlorine radicals, and sulfate radicals in aqueous-phase UV-Based advanced oxidation processes. *Water Research* **2018**, *135*, 22-30.
18. Horovitz, I.; Avisar, D.; Baker, M. A.; Grilli, R.; Lozzi, L.; Di Camillo, D.; Mamane, H., Carbamazepine degradation using a N-doped TiO₂ coated photocatalytic membrane reactor: Influence of physical parameters. *Journal of Hazardous Materials* **2016**, *310*, 98-107.
19. Starr, B. J.; Tarabara, V. V.; Herrera-Robledo, M.; Zhou, M.; Roualdès, S.; Ayrál, A., Coating porous membranes with a photocatalyst: Comparison of LbL self-assembly and plasma-enhanced CVD techniques. *Journal of Membrane Science* **2016**, *514*, 340-349.
20. Nyamutswa, L.; Zhu, B.; Navaratna, D.; Collins, S.; Duke, M., Proof of Concept for Light Conducting Membrane Substrate for UV-Activated Photocatalysis as an Alternative to Chemical Cleaning. *Membranes* **2018**, *8* (4), 122.
21. Nyamutswa, L. T.; Zhu, B.; Collins, S. F.; Navaratna, D.; Duke, M. C., Light conducting photocatalytic membrane for chemical-free fouling control in water treatment. *Journal of Membrane Science* **2020**, *604*, 118018.
22. Yan, M.; Korshin, G.; Wang, D.; Cai, Z., Characterization of dissolved organic matter using high-performance liquid chromatography (HPLC)–size exclusion chromatography (SEC) with a multiple wavelength absorbance detector. *Chemosphere* **2012**, *87* (8), 879-885.
23. Ignatev, A.; Tuhkanen, T., Monitoring WWTP performance using size-exclusion chromatography with simultaneous UV and fluorescence detection to track recalcitrant wastewater fractions. *Chemosphere* **2019**, *214*, 587-597.
24. Zhu, R.; Diaz, A. J.; Shen, Y.; Qi, F.; Chang, X.; Durkin, D. P.; Sun, Y.; Solares, S. D.; Shuai, D., Mechanism of humic acid fouling in a photocatalytic membrane system. *Journal of Membrane Science* **2018**, *563*, 531-540.
25. Rajca, M., The effectiveness of removal of NOM from natural water using photocatalytic membrane reactors in PMR-UF and PMR-MF modes. *Chemical Engineering Journal* **2016**, *305*, 169-175.
26. Cai, M.-H.; Wu, Y.-P.; Ji, W.-X.; Han, Y.-Z.; Li, Y.; Wu, J.-C.; Shuang, C.-D.; Korshin, G. V.; Li, A.-M.; Li, W.-T., Characterizing property and treatability of dissolved effluent organic matter using size

exclusion chromatography with an array of absorbance, fluorescence, organic nitrogen and organic carbon detectors. *Chemosphere* **2020**, *243*, 125321.

27. Al-Amoudi, A. S., Factors affecting natural organic matter (NOM) and scaling fouling in NF membranes: A review. *Desalination* **2010**, *259* (1), 1-10.
28. Chang, H.; Liang, H.; Qu, F.; Shao, S.; Yu, H.; Liu, B.; Gao, W.; Li, G., Role of backwash water composition in alleviating ultrafiltration membrane fouling by sodium alginate and the effectiveness of salt backwashing. *Journal of Membrane Science* **2016**, *499*, 429-441.
29. Mamane, H.; Shemer, H.; Linden, K. G., Inactivation of *E. coli*, *B. subtilis* spores, and MS2, T4, and T7 phage using UV/H₂O₂ advanced oxidation. *Journal of Hazardous Materials* **2007**, *146* (3), 479-486.
30. Bounty, S.; Rodriguez, R. A.; Linden, K. G., Inactivation of adenovirus using low-dose UV/H₂O₂ advanced oxidation. *Water Research* **2012**, *46* (19), 6273-6278.
31. Agency, E. P., Determination of Turbidity by Nephelometry. In *Method 180.1*, U.S. Environmental Protection Agency: 1993.
32. Bright, C. E.; Mager, S. M.; Horton, S. L., Predicting suspended sediment concentration from nephelometric turbidity in organic-rich waters. *River Research and Applications* **2018**, *34* (7), 640-648.
33. Her, N.; Amy, G.; Foss, D.; Cho, J.; Yoon, Y.; Kosenka, P., Optimization of Method for Detecting and Characterizing NOM by HPLC-Size Exclusion Chromatography with UV and On-Line DOC Detection. *Environmental Science & Technology* **2002**, *36* (5), 1069-1076.
34. Coble, P. G.; Spencer, R. G. M.; Baker, A.; Reynolds, D. M., *Aquatic Organic Matter Fluorescence*. Cambridge University Press: Cambridge, 2014.
35. Carstea, E. M.; Bridgeman, J.; Baker, A.; Reynolds, D. M., Fluorescence spectroscopy for wastewater monitoring: A review. *Water Research* **2016**, *95*, 205-219.
36. Sim, L. N.; Chong, T. H.; Taheri, A. H.; Sim, S. T. V.; Lai, L.; Krantz, W. B.; Fane, A. G., A review of fouling indices and monitoring techniques for reverse osmosis. *Desalination* **2018**, *434*, 169-188.
37. Amano, F.; Nakata, M.; Yamamoto, A.; Tanaka, T., Rutile titanium dioxide prepared by hydrogen reduction of Degussa P25 for highly efficient photocatalytic hydrogen evolution. *Catalysis Science & Technology* **2016**, *6* (14), 5693-5699.
38. Hurum, D. C.; Agrios, A. G.; Gray, K. A.; Rajh, T.; Thurnauer, M. C., Explaining the Enhanced Photocatalytic Activity of Degussa P25 Mixed-Phase TiO₂ Using EPR. *The Journal of Physical Chemistry B* **2003**, *107* (19), 4545-4549.
39. Livraghi, S.; Pelaez, M.; Biedrzycki, J.; Corazzari, I.; Giamello, E.; Dionysiou, D. D., Influence of the chemical synthesis on the physicochemical properties of N-TiO₂ nanoparticles. *Catalysis Today* **2013**, *209*, 54-59.
40. Shang, R.; Vuong, F.; Hu, J.; Li, S.; Kemperman, A. J. B.; Nijmeijer, K.; Cornelissen, E. R.; Heijman, S. G. J.; Rietveld, L. C., Hydraulically irreversible fouling on ceramic MF/UF membranes: Comparison of fouling indices, foulant composition and irreversible pore narrowing. *Separation and Purification Technology* **2015**, *147*, 303-310.
41. Nguyen, A. H.; Tobiason, J. E.; Howe, K. J., Fouling indices for low pressure hollow fiber membrane performance assessment. *Water Research* **2011**, *45* (8), 2627-2637.
42. Zhang, R.-X.; Braeken, L.; Liu, T.-Y.; Luis, P.; Wang, X.-L.; Van der Bruggen, B., Remarkable Anti-Fouling Performance of TiO₂-Modified TFC Membranes with Mussel-Inspired Polydopamine Binding. *Applied Sciences* **2017**, *7* (1), 81.
43. Wang, R.; Hashimoto, K.; Fujishima, A.; Chikuni, M.; Kojima, E.; Kitamura, A.; Shimohigoshi, M.; Watanabe, T., Photogeneration of Highly Amphiphilic TiO₂ Surfaces. *Advanced Materials* **1998**, *10* (2), 135-138.
44. Zuo, K.; Chen, M.; Liu, F.; Xiao, K.; Zuo, J.; Cao, X.; Zhang, X.; Liang, P.; Huang, X., Coupling microfiltration membrane with biocathode microbial desalination cell enhances advanced purification and long-term stability for treatment of domestic wastewater. *Journal of Membrane Science* **2018**, *547*, 34-42.

45. Wahab, H. S.; Bredow, T.; Aliwi, S. M., Computational investigation of the adsorption and photocleavage of chlorobenzene on anatase TiO₂ surfaces. *Chemical Physics* **2008**, *353* (1), 93-103.
46. Meng, Y.; Huang, X.; Wu, Y.; Wang, X.; Qian, Y., Kinetic study and modeling on photocatalytic degradation of para-chlorobenzoate at different light intensities. *Environmental Pollution* **2002**, *117* (2), 307-313.
47. Rosenfeldt, E. J.; Linden, K. G.; Canonica, S.; von Gunten, U., Comparison of the efficiency of OH radical formation during ozonation and the advanced oxidation processes O₃/H₂O₂ and UV/H₂O₂. *Water Research* **2006**, *40* (20), 3695-3704.
48. Ulliman, S. L.; McKay, G.; Rosario-Ortiz, F. L.; Linden, K. G., Low levels of iron enhance UV/H₂O₂ efficiency at neutral pH. *Water Research* **2018**, *130*, 234-242.
49. Chen, J.; Gu, B.; LeBoeuf, E. J.; Pan, H.; Dai, S., Spectroscopic characterization of the structural and functional properties of natural organic matter fractions. *Chemosphere* **2002**, *48* (1), 59-68.
50. Guo, L.; Santschi, P. H., Ultrafiltration and its Applications to Sampling and Characterisation of Aquatic Colloids. In *Environmental Colloids and Particles*, Buffle, J.; van Leeuwen, H. P.; Wilkinson, K. J.; Lead, J. R., Eds. 2006; pp 159-221.
51. Dow, N.; Roehr, J.; Murphy, D.; Solomon, L.; Mieog, J.; Blackbeard, J.; Gray, S.; Milne, N.; Zhu, B.; Gooding, A.; Currie, J.; Roeszler, G.; Clement, J.; Duke, M., Fouling mechanisms and reduced chemical potential of ceramic membranes combined with ozone. *Water Practice and Technology* **2015**, *10* (4), 806-813.
52. Li, X.; Li, J., Cutoff Membrane. In *Encyclopedia of Membranes*, Drioli, E.; Giorno, L., Eds. Springer Berlin Heidelberg: Berlin, Heidelberg, 2015; pp 1-2.
53. Sultana, K. A.; Islam, M. T.; Silva, J. A.; Turley, R. S.; Hernandez-Viezcas, J. A.; Gardea-Torresdey, J. L.; Noveron, J. C., Sustainable synthesis of zinc oxide nanoparticles for photocatalytic degradation of organic pollutant and generation of hydroxyl radical. *Journal of Molecular Liquids* **2020**, *307*, 112931.
54. Shen, J.-H.; Chuang, H.-Y.; Jiang, Z.-W.; Liu, X.-Z.; Horng, J.-J., Novel quantification of formation trend and reaction efficiency of hydroxyl radicals for investigating photocatalytic mechanism of Fe-doped TiO₂ during UV and visible light-induced degradation of acid orange 7. *Chemosphere* **2020**, *251*, 126380.
55. Ng, M. Characterisation and removal of natural organic matter in drinking water treatment. University of New South Wales, Australia, 2013.
56. Chin, Y.-P.; Aiken, G.; O'Loughlin, E., Molecular Weight, Polydispersity, and Spectroscopic Properties of Aquatic Humic Substances. *Environmental Science & Technology* **1994**, *28* (11), 1853-1858.

TOC Graphic

